

2017

# Studies of an unusual transthyretin protein (TTR GLU51\_SER52DUP) associated with familial amyloidosis

---

<https://hdl.handle.net/2144/23758>

*"Downloaded from OpenBU. Boston University's institutional repository."*

BOSTON UNIVERSITY  
SCHOOL OF MEDICINE

Thesis

**STUDIES OF AN UNUSUAL TRANSTHYRETIN PROTEIN (TTR  
GLU51\_SER52DUP) ASSOCIATED WITH FAMILIAL AMYLOIDOSIS**

by

**HASSAN A. ABDULLAHI**

B.S., The Ohio State University, 2014

Submitted in partial fulfillment of the  
requirements for the degree of  
Master of Science

2017



Approved by

First Reader

---

Lawreen H. Connors, Ph.D.  
Associate Professor of Pathology and Biochemistry

Second Reader

---

Maria Isabel Dominguez, Ph.D.  
Assistant Professor of Medicine

## **DEDICATION**

I would like to dedicate this work to my mother and father Ayan Hassan and Abdiwahid Abdullahi, as well as to my siblings, Mohamed, Hadia, Abdullahi, Aisha, and Adam.

## **ACKNOWLEDGMENTS**

I want to thank Dr. Lawreen H. Connors for all the advice and guidance I received over the course my time in the lab. I also want to thank Dr. Elena Klimtchuk for her knowledge and patience, as well as all the members of the Alan and Sandra Gerry Amyloid Research Laboratory. I finally want to thank Isabel Dominguez for mentoring me for the duration of my time in the program.

**STUDIES OF AN UNUSUAL TRANSTHYRETIN PROTEIN (TTR GLU51\_  
SER52DUP) ASSOCIATED WITH FAMILIAL AMYLOIDOSIS**

**HASSAN A. ABDULLAHI**

**ABSTRACT**

Transthyretin-related amyloidosis (ATTR) is a disease involving the formation of a misfolded transthyretin (TTR) protein and resulting insoluble aggregates that deposit in extracellular regions of various tissues and organs. There are hereditary forms of the disease, referred to as ATTRm, and more than 100 TTR amyloid-forming mutants have been reported.

The major goal of this work was to analyze the biochemical and biophysical properties of a unique and recently identified TTR mutant protein, TTR Glu51\_Ser52dup, found in a patient with ATTRm. Unlike other single nucleotide replacements that have been described as amyloidogenic, the gene abnormality in the present case is the first identification of a TTR duplication mutation. The patient with TTR Glu51\_Ser52dup exhibited an extremely aggressive form of ATTRm; clinical symptoms included peripheral neuropathy at baseline evaluation and rapid disease progression to early death from pneumonia and congestive heart failure. We hypothesized that the TTR Glu51\_Ser52dup variant would be less stable than the wild-type protein and similar in stability to another highly amyloidogenic mutant, TTR L55P; moreover, the highly unstable nature of this TTR variant would provide a basis for understanding the extremely aggressive clinical phenotype observed in this case.

Using *Escherichia coli* (*E. coli*) as an expression system and an appropriately modified expression vector, we produced histidine-tagged recombinant human TTR Glu51\_Ser52dup protein in high yield and purified to homogeneity. Structural and stability studies were performed by circular dichroism (CD) spectroscopy and SDS-PAGE analysis. We demonstrated that TTR Glu51\_Ser52dup was less stable than the wild-type or L55P proteins when measured under different types of denaturing conditions, including thermal and chemical stress. The presence of diflunisal, a drug that stabilizes tetrameric TTR and is currently approved for treatment of ATTRm, was also investigated; our results indicated that diflunisal stabilized the TTR Glu51\_Ser52dup protein.

Collectively, the data obtained from these studies suggest that Glu51\_Ser52dup is one of the least stable and most amyloidogenic TTR variant described to date. Future investigations are necessary to determine which specific structural elements of the protein destabilize the TTR tetramer, and precisely characterize the binding of small molecules, including diflunisal, to the protein.

## TABLE OF CONTENTS

TITLE.....	i
COPYRIGHT PAGE.....	ii
READER APPROVAL PAGE.....	iii
DEDICATION .....	iv
ACKNOWLEDGMENTS .....	v
ABSTRACT .....	vi
TABLE OF CONTENTS .....	viii
LIST OF TABLES .....	x
LIST OF FIGURES .....	xi
LIST OF ABBREVIATIONS .....	xii
INTRODUCTION .....	1
Protein Folding and Disease .....	1
Transthyretin .....	2
Amyloidosis.....	4
Transthyretin-related Amyloidosis.....	10
ATTR Treatment and Current Therapeutic Strategies .....	14
Thesis Research Objectives .....	17
METHODS.....	19

RESULTS .....	31
DISCUSSION .....	47
REFERENCES .....	50
CURRICULUM VITAE .....	57

## LIST OF TABLES

Table	Title	Page
1	Polymerase chain reaction protocol	23

## LIST OF FIGURES

Figure	Title	Page
1	Histological and ultrastructural criteria defining amyloid deposits.	8
2	TTR Fibril formation pathway	12
3	Therapeutic strategies in ATTR	16
4	Immunoblot of the patient's sera from 3 visits and the control serum	32
5	Thermal unfolding of recombinant TTRdupES	34
6	Comparison of thermal stability of TTRdupES with unstable (TTR L55P) and stable (wtTTR) variants	36
7	Heterotetramers TTRdupES and wtTTR	38
8	Thermal denaturation of TTRdupES and wtTTR mixes at different proportions	40
9	TTRdupES and wtTTR mixes at different proportions	41
10	TTRdupES, wtTTR, and L55P heated with and without diflunisal	43
11	Near UV-visible CD spectra of TTRdupES and L55P TTR	45
12	Kinetics of tertiary structure unfolding of TTRdupES and TTR L55P proteins during incubation at 80°C with and without diflunisal measured at 291 nm	46

## LIST OF ABBREVIATIONS

°C	Degrees Centigrade
µg	Micromolar
µL	Microliter
µm	Micrometer
µM	Micromolar
Aβ	Amyloid beta protein
AA	Amyloid A protein
AFM	Atomic force microscopy
AL	Immunoglobulin light chain/ Primary amyloidosis
ATTR	TTR-associated amyloidosis
ATTRm	Familial TTR-associated amyloidosis
ATTRwt	Wild-type TTR-associated amyloidosis
BCA	Bicinchoninic acid
BSA	Bovine serum albumin
CD	Circular Dichroism
Da	Dalton
ddH <sub>2</sub> O	Double distilled water
DMSO	Dimethyl sulfoxide
DNA	Deoxyribonucleic acid
dNTPs	Deoxy nucleotide triphosphates
E. coli	Escherichia coli

ELISA .....	Enzyme-linked immunosorbent assay
EtOH.....	Ethanol
FAC .....	Familial amyloid cardiomyopathy
FAP .....	Familial amyloid polyneuropathy
GAG .....	Glycosaminoglycan
Glu.....	Glutamate
H.....	Histidine
HCl .....	Hydrochloric acid
HRP .....	Horseradish peroxidase
IMAC .....	Immobilized metal ion affinity chromatography
IPTG .....	Isopropyl $\beta$ -D-1-thiogalactopyranoside
kb.....	Kilobase
kDa .....	Kilodalton
L .....	Leucine
L .....	Liter
LB .....	Lysogeny broth
M .....	Molar
MeOH.....	Methanol
mg .....	Milligram
min.....	Minute
mL .....	Milliliter
mM .....	Millimolar

NaBH.....	Sodium borohydride
NaOH .....	Histidine
ng .....	Nanogram
OD .....	Optical density
P .....	Proline
PBS .....	Phosphate buffered saline
PCR.....	Polymerase chain reaction
pg .....	Picogram
PVDF .....	Polyvinylidene difluoride
rpm .....	Revolutions per minute
SAP .....	Serum Amyloid P
SDS .....	Sodium dodecyl sulfate
Ser.....	Serine
SOC.....	Super optimal broth
SSA .....	Senile systemic amyloidosis
SSNMR .....	Solid-state nuclear magnetic resonance
TAE .....	Tris-acetate-EDTA
TEM.....	Transmission electron microscopy
TTR .....	Transthyretin
TTRdupES.....	TTR Glu51_Ser52dup
UV .....	Ultraviolet
V .....	Valine

Vis ..... Visible

wtTTR..... Wild-type TTR

## **INTRODUCTION**

### **Protein Folding and Disease**

Correct folding is essential for proper functioning of a protein; consequently, when this process is compromised, disease and injury can result. Systems exist in the organism to allow correctly folded proteins to remain, and improperly folded ones to be repaired or discarded (Stefani, 2008). The native state of the protein is achieved through a multistep pathway which includes formation of a number of intermediate folded states; these transitions have been described as a funnel-like pathway where the protein arrives at its native state and stability when the free energy of the conformation is minimized (Merlini & Bellotti, 2003). The misfolded state of a protein, caused by expression of a gene mutation or dysfunction of a normal process, is achieved in a similar fashion. The proteinopathies, such as Creutzfeldt-Jakob disease, Alzheimer's disease, Parkinson's disease, prion disease, and the systemic amyloidosis, are all examples of pathologies caused by misfolded proteins that have not been effectively refolded or discarded (Dobson, 2003).

At the cellular level, proteins are synthesized from genetic information encoded in the DNA on ribosomal complexes and transported to the endoplasmic reticulum (ER) where folding commences (Dobson, 2003). Secondary and tertiary structures arise as the protein finds a stable conformation. Chaperones aid in the process of folding by increasing the efficiency of folding, likely by

preventing competing reactions, notably aggregation (Dobson, 2003). In proteins that are partially folded or in misfolded states, hydrophobic amino acid residues may be exposed instead of buried within a protected core that excludes H<sub>2</sub>O; this causes an increased propensity of the protein to aggregate and in certain cases, can ultimately lead to amyloid fibril formation (Kim *et al.*, 2013). In the amyloid diseases, misfolded aggregates can arise either as a consequence of a genetic mutation or some other, as yet undetermined, extrinsic factor(s) that causes the precursor proteins to assume a pathologic or amyloidogenic state (Merlini & Bellotti, 2003). One such amyloid-forming protein is the plasma circulating protein, transthyretin (TTR); the misfolding, aggregation, and fibrillization of TTR is linked to the presence of mutations in coding regions of the TTR gene (familial or inherited, ATTR<sub>m</sub>) or associated with the process of aging in TTR amyloid disease featuring deposits composed of the wild-type protein (acquired, ATTR<sub>wt</sub>).

### **Transthyretin**

Transthyretin (TTR), formerly known as prealbumin, is a plasma circulating protein involved in the transport of thyroxine (T<sub>4</sub>) and retinol-binding protein attached to retinol (Cascella *et al.*, 2013). The protein is comprised of four identical subunits, each approximately 14 kDa in size; the molecular weight of the tetramer is 55 kDa. TTR is a secretory protein expressed mainly by hepatocytes and found in plasma normally at concentrations of 150-400 µg/mL (Buxbaum & Reixach, 2009). Minor sites of production include the choroid plexus and eye; in

cerebrospinal fluid, TTR levels are typically 10-40  $\mu\text{g}/\text{mL}$  (Herbert *et al.*, 1986). Each monomer of TTR is composed of 127 amino acid residues that normally fold as 8 beta strands arranged in a sandwich-like conformation of two separate, four beta strand, sheets (Azevedo *et al.*, 2013). The TTR homotetramer is extremely stable, and *in vitro* studies have shown that dissociation of the subunits requires non-physiologic conditions such as an acidic environment, elevated temperature, or chemical denaturant (Robinson and Reixach, 2014).

While the thyroid hormone, T4, is mainly transported in blood by thyroxine-binding globulin, a minor carrier of the molecule is TTR. The interaction between native state or tetrameric TTR and the ligand occurs in a binding pocket created by one of the two TTR dimer-dimer interfaces (Foss *et al.*, 2005). The energetically weaker of the two interfaces contains the hydrophobic T4 binding cavities wherein the hormone exhibits negative cooperativity once bound, making the second binding site less accessible (Johnson *et al.*, 2005). T4-binding to TTR was shown to greatly stabilize the native state of the protein (Foss *et al.*, 2005). Based on this finding, a therapeutic strategy targeting the tetrameric form of TTR was developed; consequently, the focus of much research over the past couple of decades has been the search for compounds that can selectively bind in the T4 attachment sites of TTR and prevent subunit dissociation of the protein. While many compounds have been identified, a select few have demonstrated non- or positively cooperative binding (Johnson *et al.*, 2005). One agent that effectively bound to and stabilized tetrameric TTR was the non-steroidal anti-inflammatory

drug (NSAID), diflunisal (Tojo *et al.*, 2006). Repurposed for clinical use in ATTRm, diflunisal was tested in an international, placebo-controlled study of patients with familial TTR amyloidosis featuring neuropathy; data from the two-year trial showed significant reduction of neurological indicators suggesting a slowing of disease progression (Berk *et al.*, 2013). Tafamidis, another small molecule stabilizer of native (tetrameric) TTR, has also been shown to reduce neurological progression in patients with ATTRm and has drug approval status in Europe, but not in the United States (Coelho *et al.*, 2012).

Besides being a transporter of vitamin A and thyroid hormone, TTR may have other functions in organisms. TTR levels have been recently linked to memory and cognitive functions (Fleming *et al.*, 2009). Studies have shown that TTR knock out mice have increased locomotor activity, decreased anxiety-like behaviors, spatial memory impairment, and accelerated cognitive impairment associated with aging (Sousa *et al.*, 2004; Sousa *et al.*, 2007).

### **Amyloidosis**

Amyloidosis is a term that refers to a heterogeneous group of protein misfolding diseases commonly featuring the accumulation of insoluble amyloid protein fibrils in various organs and tissues throughout the body. These pathologies can be loosely classified based on the location(s) of the amyloid deposits, either as localized with one site of involvement found close to the production of the amyloid precursor protein or systemic when multiple tissues/organs distally situated from the expression site are involved. Acquisition

of disease can be random (sporadic) or hereditary (familial), and to date, more than 30 separate human proteins have been identified as amyloidogenic (Sipe *et al.*, 2016). Some of the more commonly diagnosed forms of amyloidosis are caused by monoclonal immunoglobulin light chain (AL amyloidosis), serum amyloid A protein (AA amyloidosis), and TTR (ATTR amyloidosis) (Wechalekar *et al.*, 2016). These different forms of amyloidosis provide unique challenges in diagnosis and treatment as the disease manifestations can be quite diverse among individuals, clinical features are frequently overlapping between amyloid disease types, and in some cases, onset and progression of the disease may take many years.

Localized forms of amyloidosis include Alzheimer's disease, Parkinson's disease, Huntington's disease, and type 2 diabetes (Abedini and Schmidt, 2013). All of these feature amyloid deposits limited to a single organ; in the examples cited, the accumulation of amyloid is restricted to the brain in the first three diseases, while amyloid infiltration occurs in the pancreas in type 2 diabetes. Despite demonstration of amyloid plaque buildup in these diseases, it still is unclear whether the amyloid deposits are actually the pathological cause or an effect of the process (Pepys, 2006).

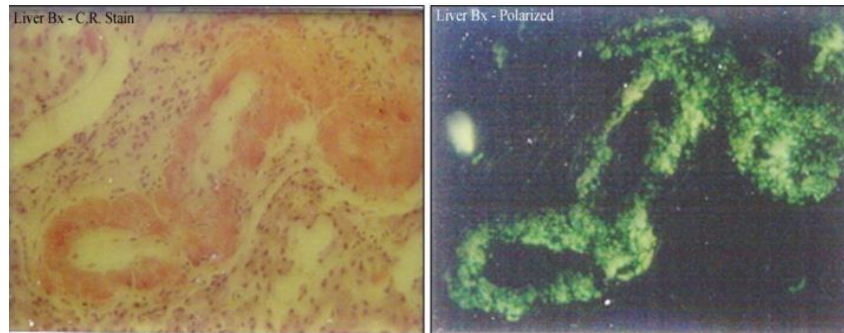
In the systemic amyloidoses, multiple organ systems and tissues are infiltrated and disrupted by the amyloid deposits. Currently, it is generally held that AL amyloidosis is the most commonly diagnosed form of amyloid disease, but other types including those associated with TTR (ATTRm and ATTRwt) are

becoming increasingly recognized (Wechalekar *et al.*, 2016). In both the AL and TTR disease types, the majority of cases feature amyloid deposits in cardiac tissue which results in cardiomyopathy and heart failure, and contributes to the highest number of patient deaths (Hoyer *et al.*, 2008). The diagnosis of amyloid in patients with myocardial amyloid deposits is usually made by cardiac MRI and right ventricular biopsy showing positive Congo red staining (Hoyer *et al.*, 2009; Sharma and Howlett, 2013). The prognosis for patients with cardiac involvement is not good especially in AL amyloidosis, as this has been reported to be the worst prognostic factor (Sharma and Howlett, 2013). Median survival is less than 6 months in untreated patients, which makes early diagnosis and treatment critical (Kyle & Gertz, 1995; Ando *et al.*, 1993). Almost every organ system is involved to some extent in cases of systemic amyloidosis including the kidneys, central and peripheral nervous system, and respiratory system. This makes it extremely difficult to diagnose and manage these diseases, as symptoms mimic many other pathological conditions.

The term “amyloid” was first used in 1853 by Rudolph Virchow who characterized unknown extracellular deposits as being “starch-like” (Virchow, 1854). Amyloid ultrastructure was first determined using electron microscopy and reported in 1959 (Cohen and Calkins, 1959). Irrespective of the fibril protein constituent, all amyloid deposits were found to have common tinctorial properties and consist of morphologically identical fibrils (**Figure 1**). These fibrils demonstrate apple-green birefringence under polarized light when stained with

Congo red and viewed by light microscopy (**Figure 1A**) (Giorgadze *et al.*, 2004). In addition, the ultrastructure of amyloid features non-branching fibrils of varying lengths (**Figure 1B**) that display an x-ray diffraction pattern consistent with an antiparallel beta-sheet configuration.

**A**



**B**

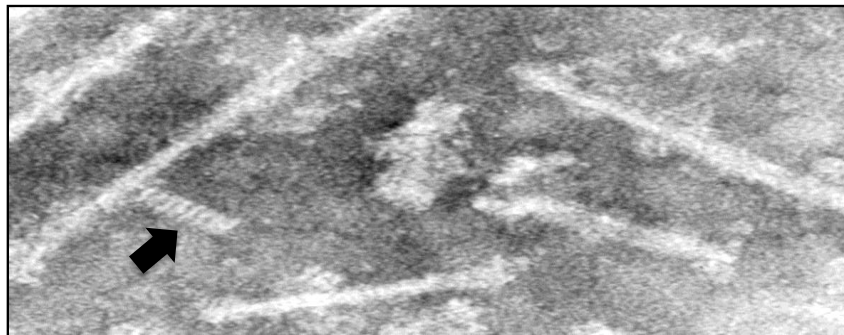


**Figure 1. Histological and ultrastructural criteria defining amyloid deposits.** (A) Congo red binding viewed by standard (left panel) and polarized (right panel) light microscopy showing positive staining and characteristic apple-green birefringence. (B) Ultrastructure featuring non-branching, variable length, ~10 nm diameter fibrils demonstrated by electron microscopy. Arrow indicates fibril associated protein, serum amyloid P-component arranged in a stacked structure.

While the demonstration of congophilia and green birefringence by light microscopy has been the gold standard for identifying amyloid deposits, newer characterization techniques have also been shown to be useful (Sipe *et al.*, 2016). *Ex vivo* or *in vitro* generated amyloid fibrils can be visualized using either transmission electron microscopy (TEM) or atomic force microscopy (AFM). Ultrastructurally, amyloid fibrils formed from variably sized proteins, i.e. polypeptide chains containing different numbers of amino acid residues, have been shown to have similar diameters (~10 nm) (Serpell *et al.*, 2000). Solid-state nuclear magnetic resonance spectroscopy (SSNMR) and x-ray crystallography techniques have greatly advanced the structural information pertaining to amyloid fibrils; the distinct morphological features of amyloid fibrils and prefibrillar forms have been elucidated through SSNMR and TEM spectroscopy, and have been found in amyloidogenic proteins such as A $\beta$  protein (Petkova *et al.*, 2005). Recent studies using fluorescence spectroscopy have proved useful in uncovering interactions between amyloidogenic proteins and cellular membranes, e.g. investigations have shown that aggregated forms of TTR increase membrane fluidity and this process has been suggested as a possible mechanism leading to cell death (Munishkina and Fink, 2007).

Amyloid deposits, in addition to the fibril protein constituent, have several non-fibrillary components that are always found in association with the deposits. These include glycosaminoglycans (GAGs) and the glycoprotein, serum amyloid P-component (SAP, see arrow in **Figure 1B**) (Wechalekar *et al.*, 2016).

Discovery of these fibril-associated components, common to all amyloid deposits, have provided diagnostic and therapeutic avenues. SAP scintigraphy is an imaging technique where radio-labeled SAP is monitored for specific organ uptake, as SAP binds to the amyloid deposits (Hazenbergh *et al.*, 2004). Eprodinate, a molecule that targets the glycosaminoglycan binding site on amyloid fibrils has been shown to slow the progression of AA amyloidosis-related renal disease (Dember *et al.*, 2007). Other specific treatments such as chemotherapy for AL amyloidosis and anti-inflammatory drugs for AA amyloidosis have also shown promise (Comenzo *et al.*, 1998; Gillmore *et al.*, 2001; Skinner *et al.*, 2004)

### **Transthyretin-related Amyloidosis**

Transthyretin-related amyloidosis (ATTR) is a systemic disease characterized by the extracellular deposition of amyloid fibrils composed of TTR. Despite having wide-ranging clinical phenotypes, ATTR is believed to have a common mechanism of amyloidogenesis. There are familial and an acquired forms of the disease; TTR amyloidosis related to mutant forms of the protein results from inherited TTR gene coding region nucleotide alterations (ATTRm) and wild-type TTR-associated amyloidosis (ATTRwt), is an age-related disease formerly known as senile systemic (SSA) or senile cardiac (SCA) amyloidosis. It is generally accepted that TTR amyloidogenesis is initiated by destabilization of the native TTR protein and dissociation of the non-covalently bound subunits to individual monomers; this is the rate-limiting step in the process (Hurshman

Babbes *et al.* 2008). Once dissociation occurs, the monomeric forms become misfolded and assume non-native conformations that favor self-aggregation; the association of misfolded subunits is likely due to exposure of hydrophobic regions which are buried deep with the properly folded protein so as to exclude H<sub>2</sub>O (Hurshman Babbes *et al.* 2008). The formation of oligomeric, pre-fibrillar forms of TTR progresses to development of amyloid filaments and ultimately, insoluble fibrils which constitute the tissue-deposited amyloid (**Figure 2**).

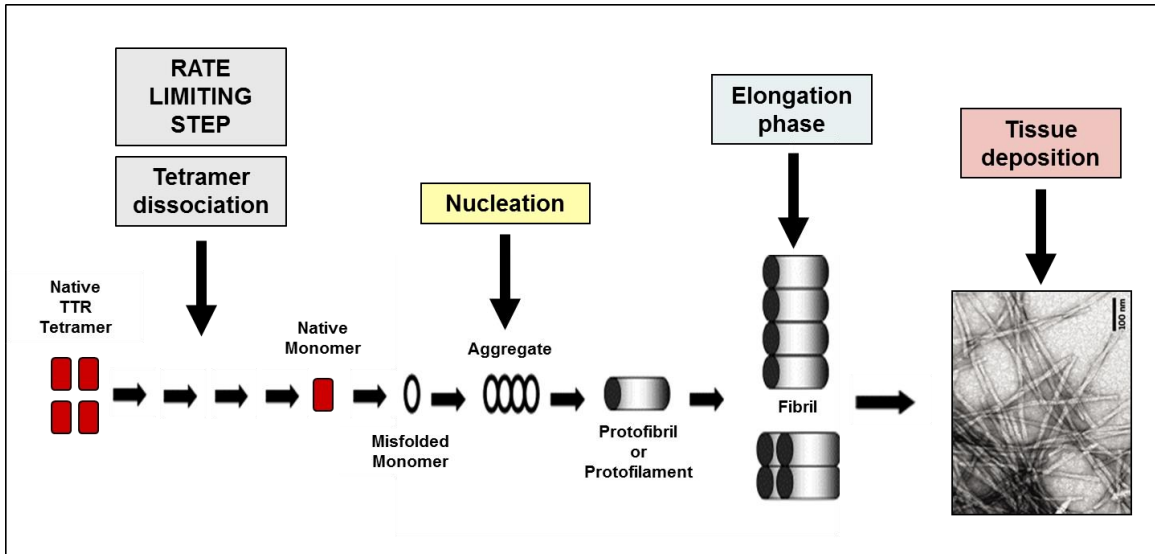


Figure 2. TTR Fibril formation pathway.

ATTRm is the most frequently occurring hereditary systemic amyloidosis; while there are endemic areas around the world, the disease is thought to occur at a prevalence of 1:1000 (de Larrea *et al.*, 2015; Ruberg and Berk, 2012). The sporadic form of the disease (ATTRwt) results from misfolding of the wild-type TTR protein in the absence of a mutation. Amyloid deposits in ATTRwt are most commonly, but not exclusively, found in the heart (Westermarck *et al.*, 1990). Cardiac amyloid deposition of wild-type TTR was reported at autopsy in a quarter of individuals over 80 years of age and found to be the cause of death in 10% of cases (Cornwell GG *et al.*, 1983; Tanskanen *et al.*, 2008).

Based on major clinical phenotype, ATTRm can be divided into TTR-related familial amyloidotic polyneuropathy (FAP) and TTR-related familial amyloidotic cardiomyopathy (FAC). FAP patients feature amyloid deposits found in various organs, but the disease manifests as symptoms of peripheral and autonomic neuropathy (Almeida *et al.*, 2004). The most prevalent amyloidogenic TTR mutant associated with FAP involves substitution of the valine residue at N-terminal position 30 with a methionine, TTR-V30M (Almeida *et al.*, 2004). Clinical onset in patients with FAP usually begins with sensorimotor peripheral neuropathy in the lower limbs and progression to sensory impairment (mainly pain/temperature sensation), as well as autonomic dysfunction including dyshidrosis, sexual impotence, gastrointestinal disturbances, and orthostatic hypotension (Ando *et al.*, 1993, Araki *et al.*, 1968). The disease was first described by a neurologist in Portugal more than 60 years ago (Andrade, 1952).

Since that initial report, patients with these clinical features have primarily been identified in Portugal, Japan, and Sweden (Conceição & De Carvalho, 2007)

One of the most aggressive, i.e. rapidly progressing, forms of ATTRm is associated with TTR L55P; this variant is the gene product of a TTR point mutation in exon 3 at codon 55 which translates to leucine replaced by proline at N-terminal residue 55 (Cardoso *et al.*, 2002). ATTRm related to L55P is a very rarely occurring disease with a clinical phenotype that features early onset in the second and third decades of life (Sousa *et al.*, 2002). *In vitro* studies using recombinantly-generated TTR L55P have demonstrated lower structural stability in the protein and more rapid formation of aggregates by this variant, compared to the wild-type and V30M proteins (Jacobson *et al.*, 1992; Kon *et al.*, 2015).

### **ATTR Treatment and Current Therapeutic Strategies**

Liver transplantation has been the main treatment option for patients with familial amyloidosis since the 1990s; the strategy is based on removing the source of the mutant TTR. Until recently, this was the major disease intervention specifically approved for patients diagnosed with ATTR, but this option is primarily for younger patients with the V30M or other non-cardiac associated mutations who are diagnosed early in the course of the disease (de Carvalho *et al.*, 2002; Herlenius *et al.*, 2004). Prior to studies with the TTR stabilizer, diflunisal, liver transplantation was the only treatment reported to halt the clinical progression of FAP (de Carvalho *et al.*, 2002).

In the past, disease management was frequently limited to utilization of drugs that controlled the symptoms patients were experiencing. However, a number of different therapeutic strategies targeting the various stages of TTR amyloid formation have provided the rationales for development and clinical testing of an assortment of agents (**Figure 3**). These potential drugs offer patients the promise of therapeutic options.

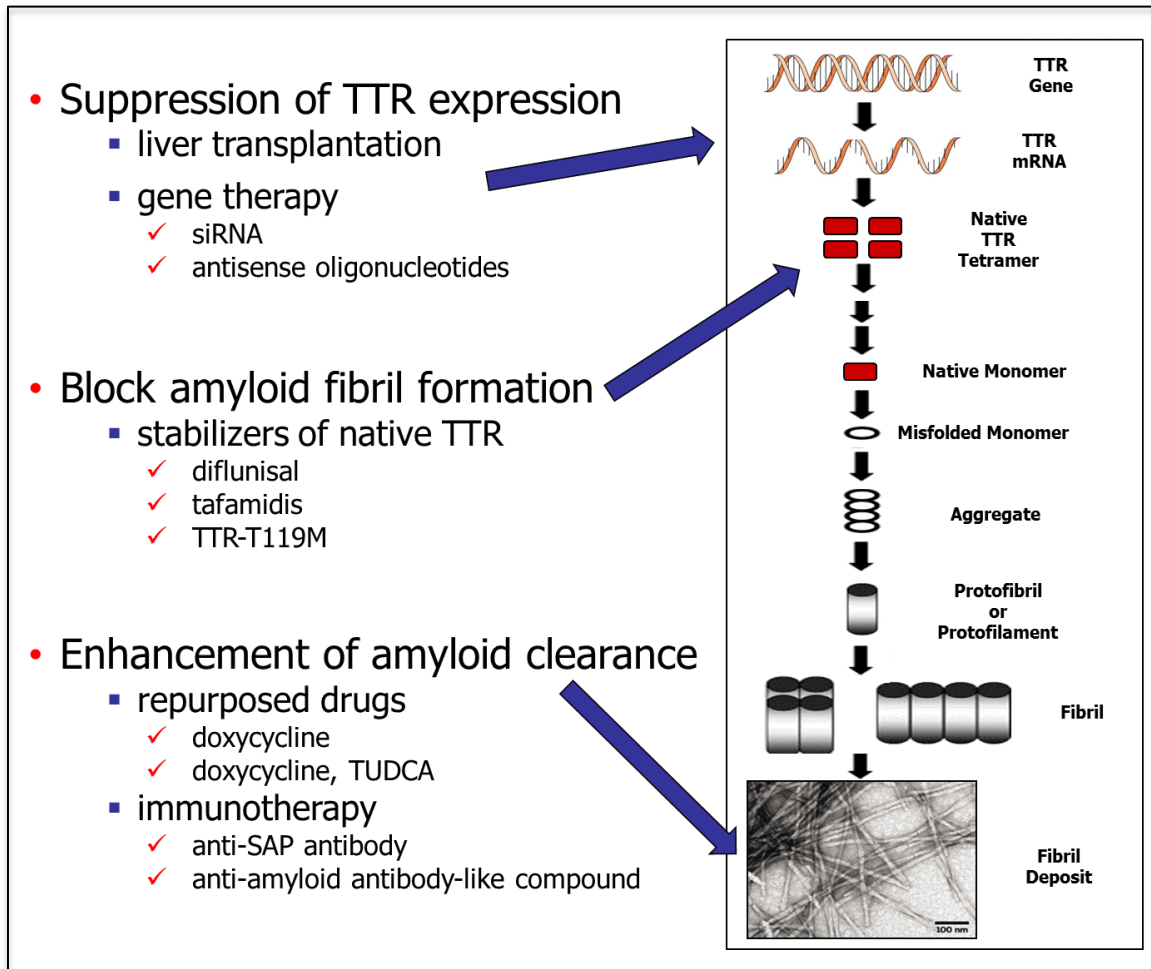


**Figure 3. Therapeutic strategies in ATTR.**

Diflunisal, a repurposed, nonsteroidal anti-inflammatory drug (NSAID), is FDA approved to treat ATTR (Berk *et al.*, 2013). Structurally similar to T4, diflunisal is believed to bind and occupy the same site on TTR that the thyroid hormone can occupy (Johnson *et al.*, 2005). Selective binding and stabilization of the TTR tetramer have been a major focus of drug development for ATTRm until most recently. Studies of patients with familial amyloidotic polyneuropathy have shown treatment with diflunisal is associated with inhibition of disease progression, and preservation of quality of life (Almeida *et al.*, 2004). Another drug, Tafamidis, has been approved for use by the European Medicines Agency. In a phase 3 clinical trial, neuropathy in tafamidis-treated patients with familial amyloidosis (V30M mutation) showed reduced progression over 18 months compared to patients treated with a placebo (Coelho *et al.*, 2012).

### **Thesis Research Objectives**

Our goals for the research detailed in this thesis were to generate a recombinant TTR protein with the novel variant sequence, Glu51\_Ser52dup, and utilize this replicate to explore the stability and structural features of this amyloidogenic protein. The mutant TTR was identified in a patient treated at the Boston University Amyloidosis Center. The mutation was associated with a severely aggressive form of familial amyloidotic polyneuropathy. A positive diagnosis of amyloidosis was established by Congo red staining of a tissue sample (abdominal fat aspirate) from the patient and the amyloid fibril protein was identified as TTR by mass spectral analysis. Based on the clinical

information, *we hypothesized that amyloidogenic TTR Glu51\_Ser52dup protein would be highly unstable compared to wild-type and other pathologic mutants.* In addition, our plan was to assess the effects of diflunisal, a kinetic stabilizer of the TTR tetramer, on the stability of the TTR mutant *in vitro.* *We postulated that diflunisal would have less of a stabilizing effect on the TTR Glu51\_Ser52dup mutant compared to native and variant forms of TTR.* Our specific aims were:

- 1) To generate recombinant TTR Glu51\_Ser52dup in high yield and purified to homogeneity for biochemical and biophysical analyses.
- 2) To measure the stability of the variant protein under denaturing conditions and compare these data to similar measurements obtained on wild-type and L55P TTR proteins.
- 3) To assess the effects of diflunisal on the stabilities of TTR Glu51\_Ser52dup, wild-type, and L55P in experiments run in parallel with those in Aim 2.

## **METHODS**

### **Chemicals and Reagents**

Primary antibody (rabbit anti-human polyclonal TTR) was purchased from DAKO (Troy, MI). Secondary antibody (HRP-conjugated, goat anti-rabbit polyclonal) was purchased from Santa Cruz Biotechnology (Dallas, TX). Glutaraldehyde and diflunisal were purchased from MP Biomedicals (Santa Ana, CA). All other materials were purchased from Applied Biosystems (Foster City, CA), Thermo Scientific (Waltham, MA), Invitrogen (Carlsbad, CA) or Sigma (St. Louis, MO), and were all of the highest grade available.

### **Clinical Samples**

All clinical samples and data used in this study were from the Boston University Amyloidosis Center serum repository with approval of the Boston University Medical Center Institutional Review Board.

### **BCA Serum Assay**

Protein concentration in the serum samples was calculated using a BCA Protein Assay kit (Thermo Scientific). BCA Protein assay relies on the reduction of copper in an alkaline medium for the colorimetric detection and quantitation of total protein. Detection is carried out at 570 nm in a spectrophotometer. Bovine serum albumin (BSA) was used as the standard protein to create a reference curve for calculating the concentration of the unknown protein. All samples and references were mapped were analyzed in a Costar 3596 cell culture plate (Sigma). The standard protein was diluted to 2000, 1500, 1000, 750, 500, 250,

125, 25, and 0  $\mu\text{g}/\text{mL}$ . Serum samples to be tested were initially diluted by a factor of 1:25 and 1:100. Ten  $\mu\text{L}$  of each diluted serum sample and 15  $\mu\text{L}$  of deionized water were combined; 25  $\mu\text{L}$  of the known BSA standard were compared as reference. To each well, 200  $\mu\text{L}$  of the working reagent was added, and the plate was shaken for 30 seconds. The plate was covered with aluminum foil and incubated at 37  $^{\circ}\text{C}$  for 30 min. The absorbance of each sample in the plate was measured at 570 nm using a CFX96 Real-Time Thermal Cycler (Bio-Rad). A standard curve was generated based on the known concentrations of the BSA standards, and was used to calculate the concentration of total protein in the serum.

### **Western Blot**

Twenty  $\mu\text{g}$  of whole serum protein per lane were analyzed by western blot, alongside a control serum sample. Twenty-five  $\mu\text{L}$  of serum sample was mixed with 40  $\mu\text{L}$  of 10% SDS and heated at 98  $^{\circ}\text{C}$  for 5 minutes. 0.88-2.5  $\mu\text{L}$  of the serum sample was added to 20  $\mu\text{L}$  of 2X Tricine sample buffer (Bio-Rad), 10  $\mu\text{L}$  of 10% SDS, and 9.12-7.5  $\mu\text{L}$  of deionized water for a total volume of 40  $\mu\text{L}$ . Samples were loaded onto a Novex 16% Tricine Protein 10 well gel (Invitrogen); a protein ladder (Spectra Broad Range Protein Ladder, Pierce) was also run on each gel.

Proteins were transferred from the gel onto a polyvinylidene difluoride (PVDF) membrane using a wet transfer method in transfer buffer (1.66 g Tris base, 7.2 g Glycine, 100 mL MeOH, total volume 500 mL, pH 8.4). The protein

transfer was done at 4 °C at 30 V overnight. The following day, the membrane was removed and placed in a blocking solution (5% dried milk in TBST) for 2 hours at room temperature. The membrane was washed 3 times in TBST and incubated with rabbit anti-human polyclonal TTR primary antibody (DAKO) at a 1:2000 dilution in 2.5% milk and TBST for 2 hours. Next, the membrane was washed again 3 times in TBST before incubation at room temperature with goat anti-rabbit HRP conjugated secondary antibody (Santa Cruz) at a 1:2000 dilution. After 1 hour, the membrane was washed 3 times in TBST and developed using ECL Plus Western Blotting Detection System (Pierce).

### **Site Directed Mutagenesis**

A synthetic human TTR gene containing altered codon usage for expression in *E. coli* cloned into the pQE-30 plasmid (Qiagen) (Kingsbury et al., 2007) was used for construction of the TTRdupES variant. Two primers containing the target mutations were designed. The gene with the appropriately modified structure (insertion of six nucleotides encoding for two amino acids, Glu51 and Ser52) was successfully constructed using QuikChange II Site-Directed Mutagenesis Kit (Agilent Technologies).

The sequences of the mutagenic primers are shown below with mutation site nucleotide insertions underlined:

(forward) 5'-CCGGTAAAACCTCCGAATCCGAATCCGGTGAACCTGCACGG-3'

(reverse) 5'-CCGTGCAGTTCACCGGATTCGGATTCGGAGGTTTTACCGG-3'.

These primers were then used for amplification of the region by polymerase chain reaction (PCR) as detailed in **Table 1**.

**Table 1: Polymerase chain reaction protocol**

Description	Amount
DNA (MK(6H)GH-TTRdupES/pQE-30), 10ng	2 $\mu$ L
10X reaction buffer	2.5 $\mu$ L
TTRdupESfor (125ng)	6.7 $\mu$ L
TTRdupESrev (125ng)	6.1 $\mu$ L
dNTPS	0.5 $\mu$ L
ddH <sub>2</sub> O	7.2 $\mu$ L
Pfu Ultra HF DNA Polymerase(2.5ng/ $\mu$ L)	0.5 $\mu$ L
Total Volume	25.5 $\mu$ L

PCR Setup:

PCR conditions		
	T (C)	Time
1	95	30 secs
2	95	30 secs
3	55	1 min
4	68	6 min
5	2-5	17 times
6	4	Forever
7	End	

The original DNA in the mixture was digested using 0.5 $\mu$ L of DpnI enzyme and incubated at 37 °C for 1 hr.

### **Plasmid DNA Gel Electrophoresis**

The presence of plasmid was confirmed by running the PCR product on a 1.2% agarose gel with a 10kb ladder. Samples were loaded and run at 150 V in TAE

buffer; the reaction product was confirmed by identifying an appropriately sized band corresponding to 3-4 kb (3.4 kb plasmid).

### **Transformation of *E. coli* XL1-Blue Supercompetent Cells**

Plasmid DNA (TTRdupES/pQE-30) was transformed into XL1-Blue cells. Fifty  $\mu\text{L}$  of XL1-Blue cells were thawed on ice for 10 minutes before 8  $\mu\text{L}$  of plasmid DNA was added and mixed with the cells. The mixture was incubated on ice for 20 minutes, heat shocked at 42 °C for 45 seconds, and incubated on ice for another 2 minutes. SOC media (400  $\mu\text{L}$ ) was added to the mixture and the tube was incubated at 37 °C for 1 hour at 250 rotations per minute. Following incubation, 200  $\mu\text{L}$  of the solution was plated on an LB plate supplemented with ampicillin (100  $\mu\text{g}/\text{mL}$ ) while the remaining 250  $\mu\text{L}$  was plated on another LB/ampicillin plate. All plates were incubated at 37 °C overnight.

### **DNA Isolation**

The plasmid DNA was isolated from the cell culture using the Wizard® Plus SV Minipreps DNA Purification System (Promega). A single colony from each plate was inoculated into a separate cell culture tube containing 5mL of LB broth and ampicillin (100  $\mu\text{g}/\text{mL}$ ). The tubes were left to incubate overnight at 37 °C with shaking at 250 rpm. The following day bacterial cells were harvested through centrifugation in a table-top microcentrifuge (top speed for 3 minutes at room temperature). The supernatant was discarded and bacterial cell pellets were re-suspended in 250  $\mu\text{L}$  of Cell Resuspension Solution. The resulting solution was transferred into a micro-centrifuge tube, 250  $\mu\text{L}$  Cell Lysis Solution was added,

and the tube was inverted 4 times to ensure complete mixing. Ten  $\mu\text{L}$  of alkaline protease was then added to the tube, the tube was inverted 4 times for complete mixing, and left at room temperature for 5 minutes. Next, 350  $\mu\text{L}$  of Neutralization Solution was added and the tube was inverted 4 times for complete mixing. The tube was centrifuged in a table-top microcentrifuge (top speed for 10 minutes) and the supernatant was pipetted onto a spin column with collection tube; the spin column was subsequently centrifuged (top speed for 1 minute) and the flow-through in the collection tube discarded and replaced. The next step involved adding 750  $\mu\text{L}$  of Wash Solution (EtOH added) to the tube followed by centrifugation (top speed for 1 minute). The flow-through was discarded and another 250  $\mu\text{L}$  of Wash Solution was added; the tube was centrifuged for 1 minute and again, the resulting flow-through was discarded. The tube was centrifuged for 2 minutes and the flow-through subsequently discarded. DNA in the spin column was finally eluted with 100  $\mu\text{L}$  of water into a clean microcentrifuge tube through centrifugation (top speed for 1 minute). The presence of plasmid in the cell culture from selected colonies was confirmed on a 1.2% agarose gel run with a 10 kb ladder. Samples were loaded and run at 150 V in TAE buffer. The reaction product was confirmed by identifying a band around 3-4 kb (3.4kb plasmid).

### **DNA Concentration Determination and Sequencing**

To determine DNA concentration, the absorbance of the collected DNA was measured at 260 nm in a Cary 300 UV-Vis spectrophotometer (Agilent). DNA

sequencing of the complete coding region in the expression plasmid was performed to verify that the correct insertion was present. Alignment of DNA sequences for wtTTR and TTRdupES are shown:

<b>TTRdupES</b> ...CCGGTAAAACCTCCGAATCC <u>GAATCC</u> GGTGAACCTGCACGG...
<b>wtTTR</b> ... CCGGTAAAACCTCCGAATCC - - - - - GGTGAACCTGCACGG...

### **Transformation into *E. coli* M15[pREP4] Cells for Expression.**

Eight  $\mu\text{L}$  of the purified plasmid DNA was added to 50  $\mu\text{L}$  of thawed M15[pREP4] cells. The mixture was incubated on ice for 20 minutes, heat shocked at 42 °C for 90 seconds, and incubated on ice for another 2 minutes. PSI broth (500  $\mu\text{L}$ ) was added to the mixture and the tube was incubated at 37 °C for 90 minutes at 250 rpm. Fifty and 100  $\mu\text{L}$  of the culture were plated on LB plates supplemented with ampicillin (100  $\mu\text{g}/\text{mL}$ ) and kanamycin (25  $\mu\text{g}/\text{mL}$ ), and the plates were incubated at 37 °C overnight.

### **Protein Expression and Purification**

The transformed *E. coli* M15 (pREP4) cells containing the recombinant TTR with N-terminal 6-histidine tags were prepared for expression. A single isolated colony from each plate was inoculated into test tubes containing 4.5 mL of LB broth supplemented with ampicillin (100  $\mu\text{g}/\text{mL}$ ) and kanamycin (25  $\mu\text{g}/\text{mL}$ ). The test tubes containing the cell cultures were incubated at 37 °C with shaking at 225 rpm. The next day, four flasks were prepared, each containing the cell cultures

inoculated into 500 mL of autoclaved LB broth supplemented with ampicillin (100 µg/mL) and kanamycin (25 µg/mL). The flasks containing the mixtures were incubated at 37 °C with shaking at 225 rpm for 3 hours until the optical density (OD) exceeded 0.6 at 600 nm. Next, 500 µL (for a final concentration 1mM) of β-D-1-thiogalactopyranoside (IPTG) was added to each flask to induce expression of the recombinant TTR protein. After an additional 4 hours of incubation under the same conditions, the mixtures were centrifuged in a SLA-1500 rotor at 6,000 rpm for 20 minutes at 4 °C. The supernatants were discarded and the cell pellets were stored overnight at -20 °C.

The pellets were thawed on ice for 15 minutes before being re-suspended in immobilized-metal ion affinity column (IMAC) cell lysis buffer at 3 mL per gram wet weight. The resulting solution was supplemented with lysozyme (1 mg/mL) and was incubated on ice for 30 minutes. Next, the cells were sonicated in bursts on ice to avoid overheating until the solution appeared transparent. The solution was then centrifuged in a SS-34 rotor at 9,000 rpm for 30 minutes at 4 °C. Supernatant was transferred into 50 mL conical tubes with a syringe containing a 0.22 µm filter.

A 6 mL Nickel-Nitriloacetic Acid (NTA) Agarose column (Qiagen) was prepared and equilibrated with IMAC wash buffer. Twenty mL of the supernatant was loaded and allowed to flow through the column into a collection tube. The column was rinsed several more times with IMAC wash buffer until the optical density (OD) reading at 280 nm was zero. The recombinant TTR protein was

then eluted in IMAC elution buffer; the eluted samples with OD > 0.1 at 280 nm were combined. Isolated protein samples were dialyzed against 50% PBS solution using a 7,000 MWCO Slide-A-Lyzer cassettes (Thermo Scientific) for 3 hours, changing the PBS every 30 minutes.

The amount of purified recombinant TTR with N-terminal 6-histidine tag was determined by measuring the absorbance of the dialyzed solution at 280 nm. The dialyzed protein solution was aliquoted into small vials, flash frozen in a combination of dry ice and acetone, and stored at -150 °C until required for analysis.

### **Subunit Exchange Procedure**

The recombinant wild-type and recombinant mutant (TTR-Glu51\_Ser52dup) were mixed in varying amounts (3:1, 1:1, 1:3 ratios) at a total working TTR concentration of 0.2 mg/mL. Mixtures were incubated at 4 °C for 48 hours to allow for subunit exchange (Schneider, Hammarstrom, Kelly, 2001) and cross-linked with glutaraldehyde following the protocol described below.

### **Transthyretin – Diflunisal Samples**

Diflunisal (MP Biomedicals) was dissolved in a solution of 0.1% DMSO and 9.9% EtOH in deionized water to make a 10X stock solution (3.6 mM). Recombinant TTR tetramer (0.2 mg/mL equivalent to 3.6 μM) was pre-incubated with 100 molar excess of diflunisal (0.36 mM) for 2 hours at room temperature.

### **Transthyretin Aggregation Studies**

TTR samples with and without diflunisal were incubated in glass vials at 80 °C for

0-24 hours. Aliquots were taken at time points during the incubation (0, 1, 2, 4, 24 hours), cross-linked with glutaraldehyde, and analyzed by SDS-PAGE analysis as detailed in the next section.

### **Protein Cross-Linking Procedure**

Five  $\mu\text{L}$  of 25% glutaraldehyde was added to 20  $\mu\text{L}$  of protein sample and incubated at room temperature for 4 minutes. The reaction was quenched with 5  $\mu\text{L}$  of 7%  $\text{NaBH}_4$  in 0.1 M  $\text{NaOH}$ .

### **Sodium Dodecyl Sulfate Polyacrylamide Gel Electrophoresis Analysis**

Protein samples were mixed with 2X non-reducing sample loading buffer (125 mM Tris-HCl, pH 6.8, 20% glycerol, 4% SDS, 0.1% bromophenol blue). The mixtures were boiled for 5 minutes before being loaded into 1 mm wells on a 8-16% Tris-Glycine or 16% Tricine gel (Invitrogen) with a protein ladder standard (Pierce) as reference. Protein bands were visualized after developing the gel in GelCode Blue Stain Reagent (Thermo Scientific) for 2 hours.

### **Phast Gel Analysis**

Glutaraldehyde cross-linked protein samples were mixed with 2X non-reducing sample loading buffer and boiled for 5 minutes employing the method described previously. Using the automated Pharmacia Phast System (GE, Fairfield, CT), samples were loaded onto a 10-15% Gradient pre-cast gel with SDS buffer strips located at both ends of gel.

### **Circular Dichroism Spectroscopy**

Circular dichroism (CD) spectral data was obtained on a Jasco J-815 spectro-

polarimeter equipped with a thermoelectric temperature controller. Near UV (330-250 nm, 1 nm bandwidth) and far UV (250-190 nm, 1 nm bandwidth) data were collected in 10 mm and 1 mm path length quartz cells, respectively. Far UV CD spectral data were smoothed using Jasco noise reduction routine and normalized to protein concentration. CD data are presented as mean residue molar ellipticity (MRE) values. Protein sample solutions were prepared at 0.2 mg/mL in PBS. To measure thermal stability, protein samples were heated from 25 °C to 98 °C at 0.1 °C/min or 1 °C/min measured at 215 and 220 nm.

## RESULTS

*Serum samples from the patient with TTR Glu51\_Ser52dup mutation show lower levels of transthyretin protein compared to control sample*

With the focus of the study on the characterization of a novel amyloidogenic TTR, we analyzed the serum samples from the patient for whom this novel mutation was identified. A western blot analysis of patient sera collected during three consecutive visits to the clinic in 2010, 2011, and 2012 confirmed the presence of the TTR protein in all samples (**Figure 4**). Analysis of the cross-linked sera indicated the presence of TTR in the native tetrameric state (55 kD), as well as higher molecular weight species of complexed TTR. Serum TTR (prealbumin) concentrations, assessed through nephelometric analysis in the Boston Medical Center Pathology Clinical Laboratory, showed lower amounts of TTR in the patient samples compared to the control. For the patient at baseline and two annual follow-up visits, the serum TTR concentrations were 11 mg/dL in 2010, 17 mg/dL in 2011, and 5 mg/dL in 2012 mg/dL; the control serum demonstrated a TTR level of 28 mg/dL. The patient TTR levels are below the range reported for healthy individuals (18-45 mg/dL, Buxbaum and Reixach, 2009). This finding is consistent with the literature as patients with ATTRm have typically been found to have lower serum levels of TTR, which is even more pronounced with progression of disease (Buxbaum *et al.*, 2010).

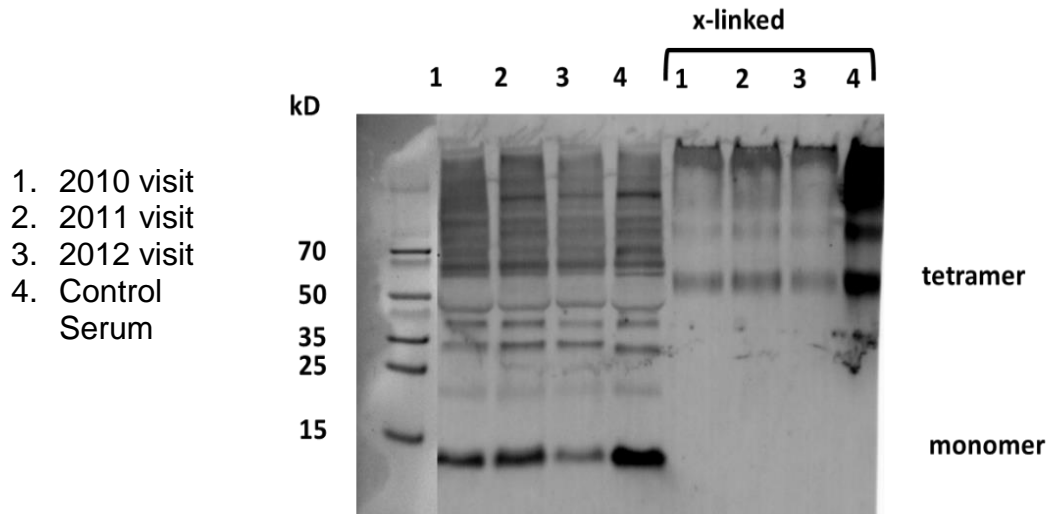


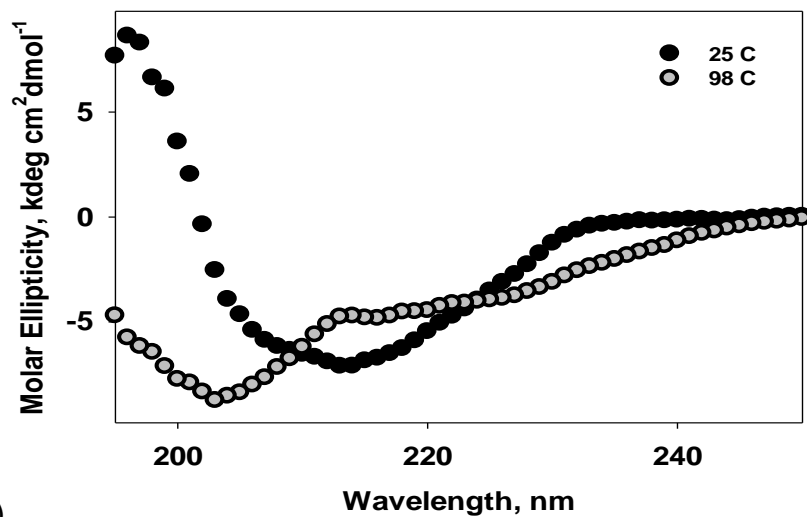
**Figure 4. Immunoblot analysis of patient sera from baseline and 2 annual follow-up evaluations.** Original serum samples and samples cross-linked with glutaraldehyde were evaluated. Total protein concentration in serum was measured by BCA assay; serum samples with the same amount of total protein were subjected to SDS-PAGE followed by immunoblotting with primary (rabbit anti-human TTR) and secondary (goat anti-rabbit IgG-HRP) antibodies.

*Recombinant TTRdupES is less stable compared to wild-type and L55P TTR*

Our aim was to study the effect of the two amino acid insertion found in TTR Glu51\_Ser52 on the structure, stability, and aggregation properties of the protein. Thus, we developed recombinant versions of the mutant, TTRdupES, and used these replicates in our biochemical and biophysical analyses. In addition, recombinant wild-type and L55P mutant TTR were produced and used to compare the unfolding and aggregation propensities of these proteins.

The thermal stabilities of wild-type, TTRdupES, and L55P TTR were examined by using CD spectroscopy (**Figure 5A**). All CD measurements were obtained on TTR samples solubilized in phosphate buffer (pH 7.4) at a protein concentration of 0.2 mg/mL, a level within the physiological range of healthy subjects (Buxbaum & Reixach, 2009). The far-UV spectrum obtained for TTRdupES at 25 °C shows the predominantly  $\beta$ -structured native conformation of TTR. Heating to 98 °C caused marked losses in the protein secondary structure. The ordered  $\beta$ -sheet structure was presumed to adopt a non-native random coil shape. Due to observable differences in CD spectra at 25 °C and 98 °C, the wavelengths of 220 nm and 215 nm were selected for monitoring of the protein thermal denaturation. Far UV CD at 220 nm for  $\beta$ -sheet to random coil conversion was recorded during sample heating from 25 °C to 98°C at different heating rates. The difference in slow (0.1 °C/min) and fast (1 °C/min) melt unfolding of the protein demonstrates the rate-dependent shift in melting transitions (**Figure 5B**).

(A)



(B)

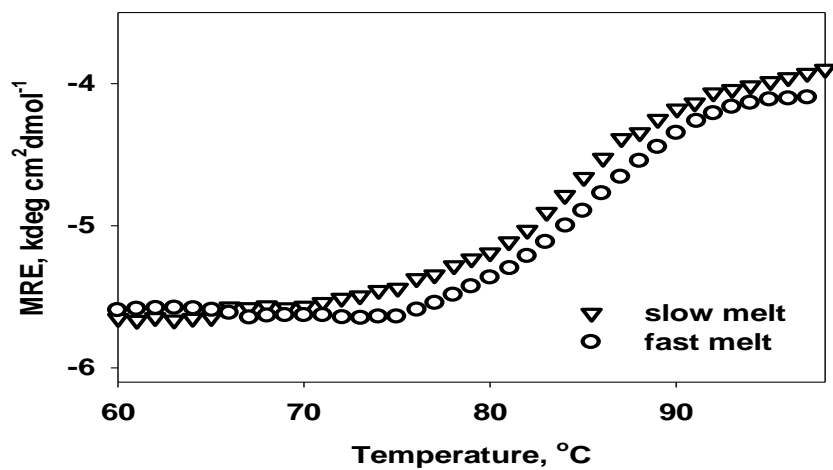


**Figure 5. Thermal unfolding of recombinant TTRdupES.** (A) Far UV CD spectra of intact TTR recorded at 25 °C and of the same protein that was heated to 98 °C. (B) CD melting data recorded at 220 nm during protein heating at fast (1 °C/min) and slow (0.1 °C/min) rates.

The far-UV spectra for the amyloidogenic mutants, TTRdupES and L55P TTR, as well as the wild-type are compared in **Figure 6A**. The spectra show a very high degree of similarity in secondary structure for all three proteins. Monitoring of the CD signal at 215 nm during sample heating from 25 °C to 98 °C allowed us to compare the transition between the folded and unfolded state for the wild-type, TTRdupES, and L55P TTR proteins (**Figure 6B**). For the thermal denaturation experiment, each sample was initially pre-incubated in 3M urea to destabilize the protein and facilitate an earlier transition into the unfolded state. This allowed us to visualize the entire unfolding process for all proteins involved, as the wild-type TTR protein has a melting temperature exceeding 98 °C (Colon and Kelly, 1992). In this study, we observed a significant difference in the melting temperatures of the proteins with TTRdupES < L55P TTR < wild-type TTR. This earlier transition into the unfolded state demonstrates that TTRdupES is destabilized more easily than the wild-type, and even more than the highly aggressive L55P TTR variant (Jacobson *et al.*, 1992; Kon *et al.*, 2015).

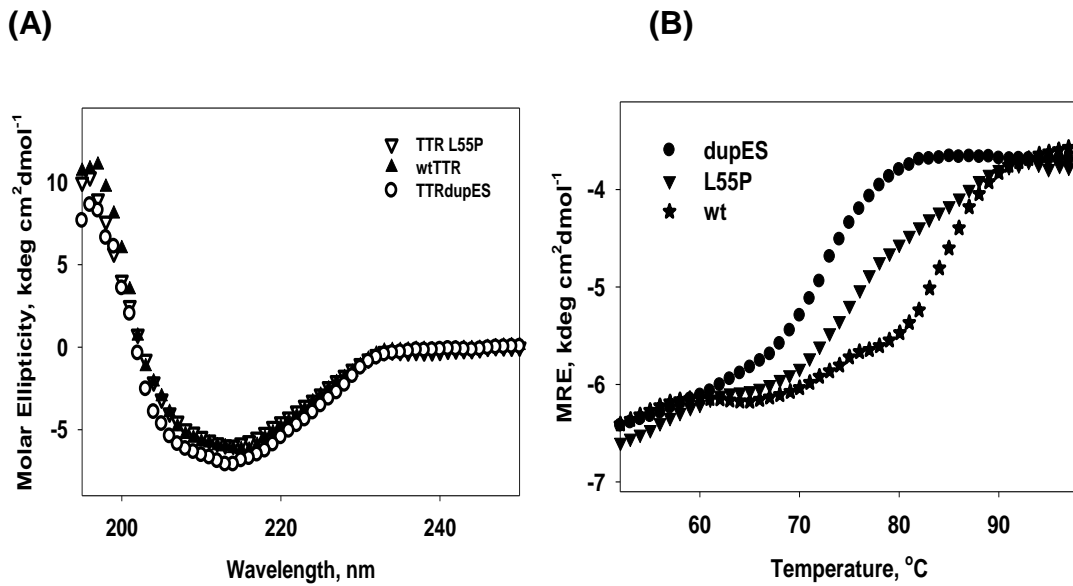


**Figure 6. Comparison of the thermal stabilities of TTRdupES, L55P (an unstable variant) and wild-type proteins (stable TTR).** Thermal unfolding of recombinant TTRdupES, L55P, and wild-type TTR proteins were individually analyzed by CD; samples were pre-incubated in 3 M Urea. **(A)** Far UV CD spectra of intact proteins recorded at 25 °C. **(B)** CD melting data recorded at 215 nm during protein heating at a slow (0.1 °C/min) rate.

*Analyses of TTRdupES and wild-type TTR, and heterotetramers of the proteins show decreased stability with increasing ratio of TTRdupES*

In most of the ATTRm patients, wild-type and amyloidogenic mutant TTR proteins are co-expressed, i.e. patients are heterozygous for the TTR gene mutation (Schneider, Hammarstrom, Kelly, 2001). In order to study the effect of the TTRdupES on the formation and stability of TTR heterotetramers, we performed the following studies. The TTRdupES and wild-type TTR proteins were mixed at different ratios and pre-incubated at 4 °C for 48 hours to allow for subunit exchange and the formation of heterotetramers (Schneider, Hammarstrom, Kelly, 2001). Homotetramers of TTRdupES and wild-type TTR were concurrently incubated during that time period, and after 48 hours all samples were cross-linked with glutaraldehyde. Our electrophoretic analysis showed that wild-type TTR is present almost completely in the tetrameric state (55 kD); this observation demonstrates the high structural integrity of the sample (**Figure 7**). However, as the number of TTRdupES subunits increases in the heterotetramers, we observe a gradual diminishing in the native (tetrameric) state of the protein; lower molecular weight forms of TTR become easily identifiable in the more anodal region of the gel when the proportion of TTRdupES to wild-type TTR is 2:2 and 3:1. Thus, we conclude that increasing the number of TTRdupES subunits causes the TTR tetramers to dissociate into monomeric (14 kD) and dimeric (30 kD) forms.

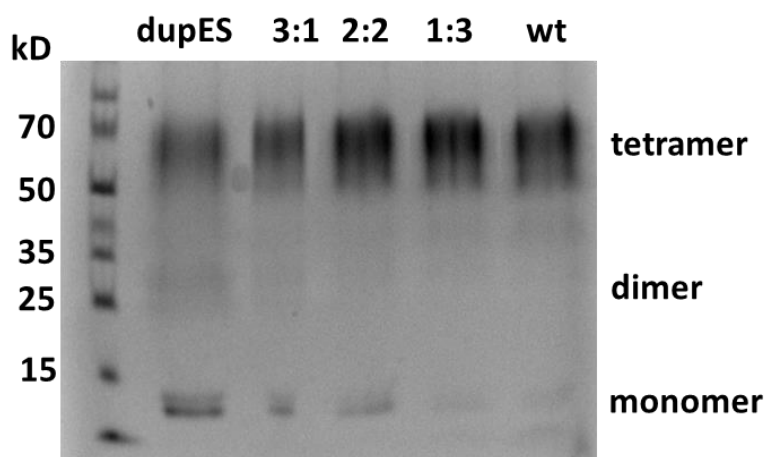


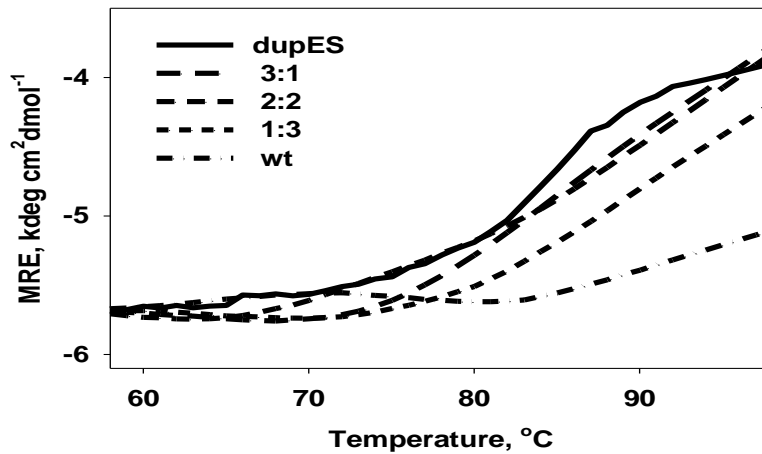
**Figure 7. Electrophoretic analysis of TTRdupES and wild-type TTR**

**heterotetramers.** Recombinant TTRdupES and wild-type TTR proteins were mixed at different ratios. Samples were pre-incubated at 4 °C for 48 hrs, cross-linked with glutaraldehyde, subjected to SDS-PAGE, and stained with Coomassie Blue.

Thermal denaturation of TTRdupES, wild-type TTR, and mixtures of the two proteins in physiological conditions was measured by far-UV CD spectroscopy (**Figure 8A**). In a separate experiment, the samples were initially pre-incubated in 4.5 M urea to destabilize and facilitate transition, and to visualize the entire unfolding process (**Figure 8B**). The mixtures of wild-type TTR and TTRdupES exhibit cooperative transition which confirms the initial heterotetramer formation after pre-incubation of two variants. Heterozygous protein denaturation can occur gradually (cooperatively) or happen in more than one transition state (Clark, 2005). Observed cooperative transition likely indicates that subunit exchange did occur. The heterotetramers undergo thermal unfolding at significantly lower temperatures compared to pure wild-type TTR tetramer (> 98 °C). This finding demonstrates that the presence of even one TTRdupES mutant subunit in the heterotetramer (TTRdupES: wtTTR is 1:3) is sufficient for major destabilization of the entire tetramer.

The SDS-PAGE analysis of TTR homo- and heterotetramers, heated to 80 °C, showed a decrease of tetrameric state (55 kD) within 4 hours with a coincident increase in dimeric (30 kD) and monomeric (14 kD) forms of TTR (**Figure 9**). This effect is more pronounced in mixtures with a high content of the TTRdupES illustrating the characteristic instability of the mutant protein.

(A)



(B)

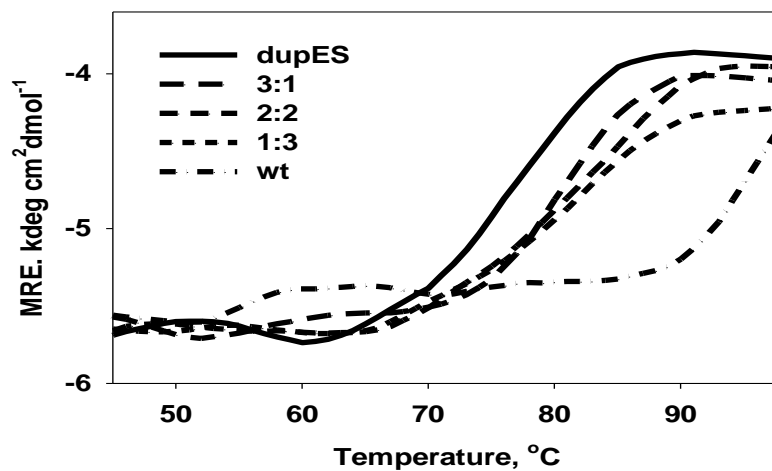


**Figure 8. Thermal denaturation of TTRdupES and wild-type TTR mixtures.**

Protein sample mixtures of TTRdupES and wild-type TTR were pre-incubated at  $4^{\circ}\text{C}$  for 48 hours to allow formation of heterotetramer. Samples were (A) slowly ( $0.1^{\circ}\text{C}/\text{min}$ ) heated in PBS or (B) pre-incubated in 4.5 M urea for 1 hour and heated at the rate of  $1^{\circ}\text{C}/\text{min}$ . CD melting data were recorded at 220 nm during protein heating.

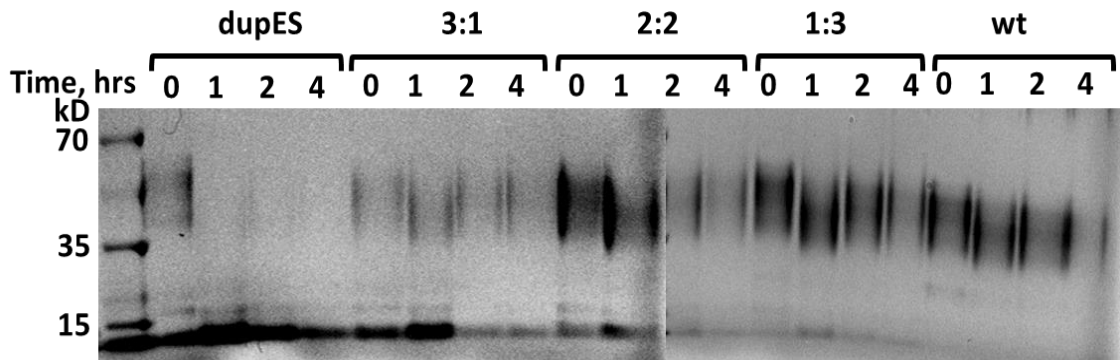


**Figure 9. Electrophoretic analysis of TTRdupES and wild-type TTR mixtures.** TTRdupES and wild-type TTR proteins were pre-incubated at 4 °C for 48 hours to form heterotetramers. The samples were subsequently incubated at 80 °C with shaking at 200 rpm. At indicated time points samples were cross-linked with glutaraldehyde and subjected to SDS-PAGE followed by Coomassie staining.

*Diflunisal stabilizes the quarternary structures of TTRdupES, TTR L55P, and wild-type TTR proteins*

Diflunisal is a non-steroidal anti-inflammatory drug (NSAID) repurposed to treat patients with FAP amyloidosis. We investigated the stabilizing effect of diflunisal on recombinant TTRdupES under stress conditions. TTRdupES, wild-type TTR, and L55P TTR, in the presence and absence of diflunisal at a 100 molar excess of drug, were incubated at 80 °C for 24 hours. Samples were cross-linked before and after incubation (**Figure 10**). Diflunisal, pre-incubated with TTRdupES (time point 0), appears to stabilize the native tetrameric state of the protein shifting the equilibrium from the monomeric (14 kD) and dimeric (30 kD) forms to the tetrameric (55 kD) state. After 24 hours at 80 °C, the tetrameric form of TTRdupES in the absence of diflunisal is dissociated and the high molecular weight oligomeric species are formed; however, TTRdupES incubated with diflunisal preserves the tetrameric state of the protein. For the wild-type and L55P TTR proteins, when diflunisal is absent, the tetramers (55 kD) begin to dissociate into dimers (30 kD) and monomers (14 kD) after 24hrs of incubation; conversely, the presence of diflunisal prevents the tetramer dissociation of both the wild-type and L55P proteins. Interestingly, the stabilizing effect of diflunisal appeared to be much more pronounced on the conformation of the TTRdupES mutant compared to wild-type and L55P TTR.

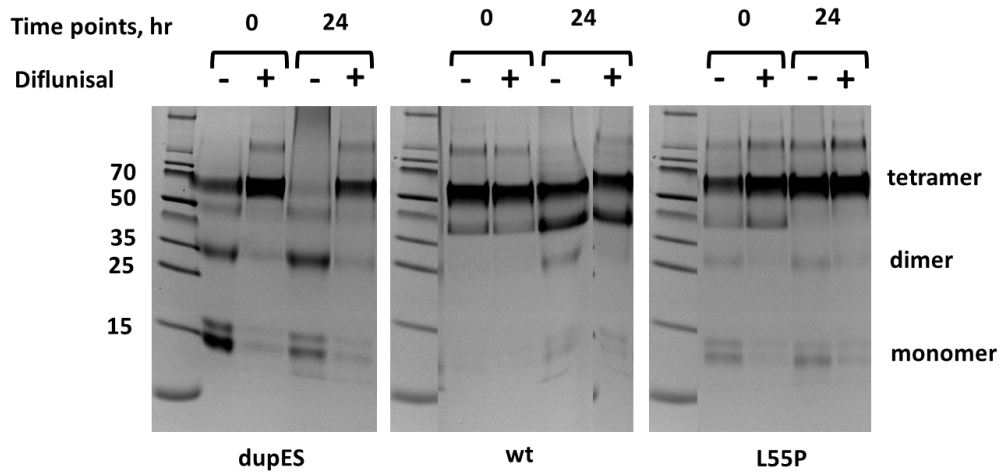


**Figure 10. TTRdupES, wild-type TTR, and L55P TTR heated in the presence and absence of diflunisal.** Proteins were pre-incubated with and without diflunisal in PBS for 2 hours at 25 °C; all samples were subsequently incubated at 80 °C with shaking at 200 rpm for 24 hours, cross-linked with glutaraldehyde, and subjected to SDS-PAGE followed by Coomassie staining.

To further explore the stabilizing effect of diflunisal on the TTR tetramers, we compared unfolding of TTRdupES and L55P TTR in the presence and absence of the drug. The near-UV CD spectra were recorded while the samples were incubated at 80 °C over the course of 60 minutes (**Figure 11**). Changes in the CD signal with a maximum at 291 nm corresponding to the Trp79 residue reports directly on the changes in the tertiary structure of the monomer upon heating (Kelly *et al.*, 2005). TTRdupES unfolds much faster and to a higher degree than L55P TTR (**Figure 11A and 11B**). Both TTRdupES and L55P TTR elicited positive responses to diflunisal (**Figure 11C and 11D**). The kinetics of the protein unfolding process is shown by plotting the values of the CD signals at 291 nm against the time points (**Figure 12**). The comparison of protein unfolding kinetics demonstrates that TTRdupES exhibits a greater overall recovery in CD signal upon the addition of diflunisal.

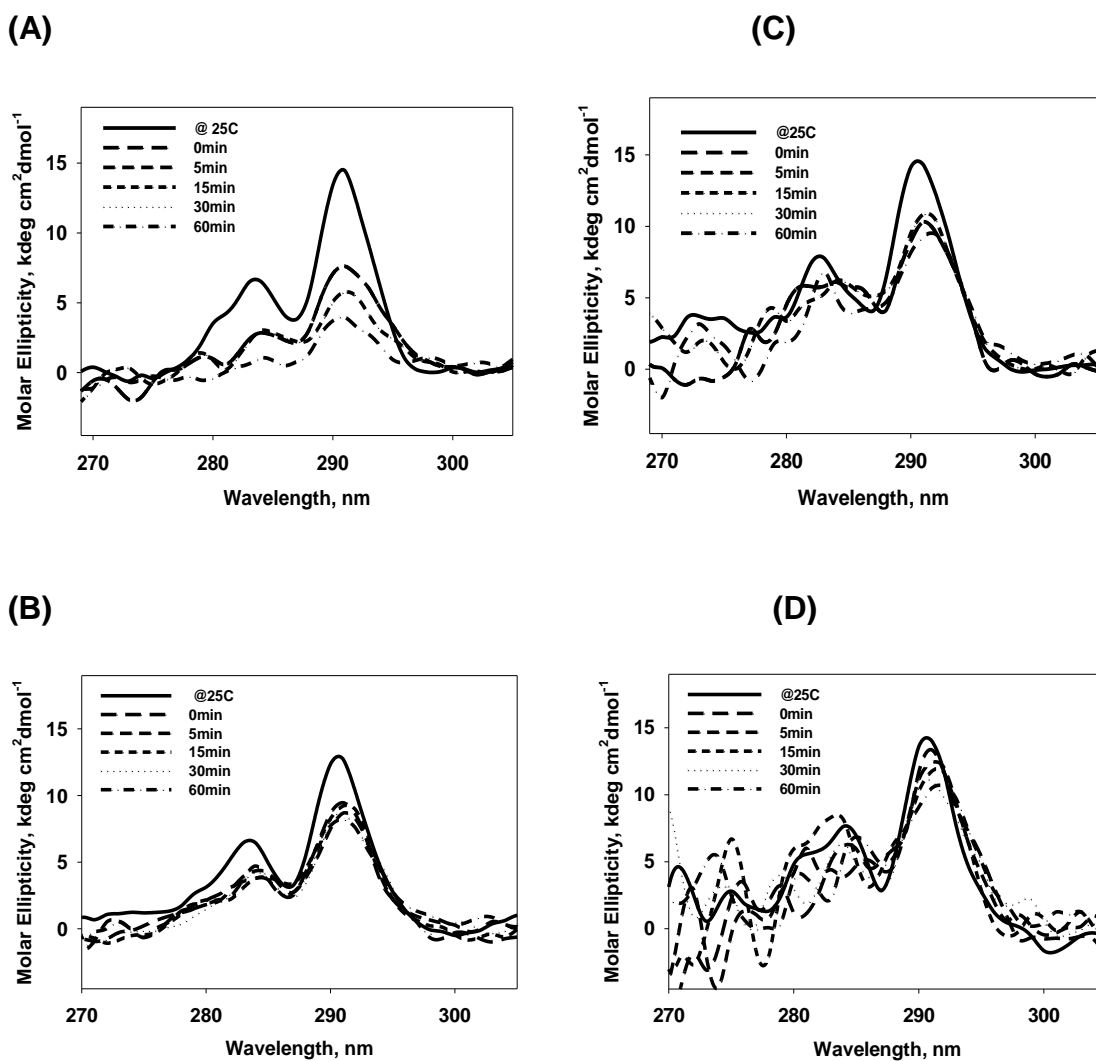


**Figure 11. Near UV-visible CD spectra of TTRdupES and L55P TTR in the presence and absence of diflunisal.**

(A) TTRdupES, (B) TTR L55P, (C) TTRdupES with diflunisal, and (D) TTR L55P with diflunisal recorded during heating at 80 °C.

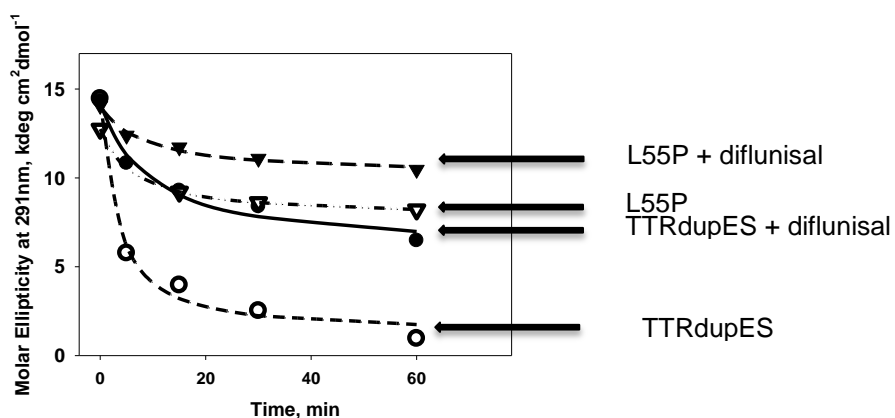


**Figure 12. Kinetics of tertiary structure unfolding of TTRdupES and L55P TTR in the presence and absence of diflunisal.** Samples were incubated at 80 °C with and without diflunisal and removed at time intervals between 0 and 60 minutes for CD measurements at 291 nm. The CD data from signals obtained at 291 nm were plotted against the individual time points.

## DISCUSSION

Analysis of patient serum from initial and follow-up clinical evaluations confirmed the presence of tetrameric TTR in all three samples. Compared to control serum, the levels of TTR were markedly lower in the patient with TTRdupES variant at all visits. This finding is consistent with published reports showing that patients with ATTRm have been found to have lower TTR serum levels compared to healthy individuals (Chan *et al.*, 2017). It is not completely understood why serum TTR levels are reduced in patients with ATTRm, but several mechanisms have been proposed. These include the possibility of higher clearance of mutant protein, reduced liver secretion in response to higher misfolded TTR load, and less likely cytokine suppression of TTR transcription in the presence of chronic inflammation secondary to autonomic neuropathy (Buxbaum *et al.*, 2010).

One of the goals of the present study was to generate a recombinant TTR protein with the newly discovered mutation of interest (TTR Glu51\_Ser52), and to characterize the biophysical properties of the protein, as well as compare these biophysical data to those obtained on wild-type TTR and the most unstable amyloidogenic variant, TTR L55P. Our results from SDS-PAGE analysis of TTR tetramer stability, under varying conditions and at different time intervals, indicated that the TTR Glu51\_Ser52dup mutant is substantially more unstable than the wild-type protein or even the L55P TTR mutant. Loss of tetrameric state was identifiable within 1 hour when the Glu51\_Ser52dup mutant protein was

subjected to heat denaturing conditions (80 °C). Heterotetramers formed by subunit exchange in mixtures of the wild-type and TTRdupES showed that the stability of the tetramers decreased with increased amounts of the mutant. This suggests that subunits of the mutant have an overall destabilizing effect on wild-type monomers when present together in tetrameric form as likely would be the case in a patient heterozygous for the amyloidogenic mutation. Comparison of TTRdupES to the L55P TTR mutant in our biophysical and biochemical studies was important as the latter protein is considered to be the most unstable and amyloidogenic of all TTR proteins (Kon *et al.*, 2015). ATTRm associated with L55P TTR is reported to be a very aggressive form of amyloid disease, and interestingly, our data suggest that TTRdupES was less stable.

Circular dichroism analysis demonstrated the marked difference in stability between wild-type TTR and the TTRGlu\_51Ser52dup mutant. Thermal denaturation demonstrated a decreased stability of the mutant, with the protein unfolding at lower temperatures compared to the wild-type and L55P TTR. Also, the unfolding was evident in a very short time interval. The loss of native structure was observed in the near UV wavelength range, a wavelength interval that can be used to observe changes in the structural environment of aromatic amino acid side chains (Kelly *et al.*, 2005). These residues include tryptophan, tyrosine, and phenylalanine which are all present in the TTR polypeptide chain. Tryptophan has a peak absorbance at approximately 290 nm where we observed greater structural changes in the TTRdupES protein compared to TTR L55P

(Kelly and Price, 2000). Although CD monitoring the near UV wavelength range may not be able to tell us about the overall structure of a protein, it does provide information when comparing two or more variants of the same protein (Kelly *et al.*, 2005). Stabilization of all TTR proteins was observed when each was incubated with the TTR tetramer stabilizing drug, diflunisal; the effects seemed most dramatic with the TTRdupES protein.

In summary, results of the studies reported in this thesis demonstrate that the recombinant TTR variant protein, Glu51\_Ser52dup, is less stable *in vitro* compared to recombinant wild-type TTR, as well as the amyloid-forming TTR mutant, L55P. Future studies of the structural dynamics, as well as the binding kinetics are required to more fully understand the amyloidogenic nature of the mutant protein and the relationship of the two inserted amino acid residues on the molecular structure of this highly unstable TTR protein variant.

## REFERENCES

- Abedini, A., & Schmidt, A. M. (2013). Mechanisms of Islet Amyloidosis Toxicity in Type 2 Diabetes. *FEBS Letters*, *587*(8), 1119–1127.  
<https://doi.org/10.1016/j.febslet.2013.01.017>
- Almeida, M. R., Macedo, B., Cardoso, I., Alves, I., Valencia, G., Arsequell, G., ... Saraiva, M. J. (2004). Selective binding to transthyretin and tetramer stabilization in serum from patients with familial amyloidotic polyneuropathy by an iodinated diflunisal derivative. *Biochemical Journal*, *381*(2), 351–356.  
<https://doi.org/10.1042/BJ20040011>
- Ando, Y., Araki, S., & Ando, M. (1993). 3. Transthyretin and Familial Amyloidotic Polyneuropathy. *Internal Medicine*, *32*(12), 920–922.  
<https://doi.org/10.2169/internalmedicine.32.920>
- Ando, Y., Nakamura, M., & Araki, S. (2005). Transthyretin-Related Familial Amyloidotic Polyneuropathy. *Archives of Neurology*, *62*(7), 1057–1062.  
<https://doi.org/10.1001/archneur.62.7.1057>
- Andrade, C. (1952). A peculiar form of peripheral neuropathy; familiar atypical generalized amyloidosis with special involvement of the peripheral nerves. *Brain: A Journal of Neurology*, *75*(3), 408–427.
- Araki, S., Mawatari, S., Ohta, M., Nakajima, A., & Kuroiwa, Y. (1968). Polyneuritic Amyloidosis in a Japanese Family. *Archives of Neurology*, *18*(6), 593–602.  
<https://doi.org/10.1001/archneur.1968.00470360015001>
- Azevedo, E., Silva, P. F., Palhano, F., A. Braga, C., & Foguel, D. (2013). Transthyretin-Related Amyloidoses: A Structural and Thermodynamic Approach. <https://doi.org/10.5772/53148>
- Berk, J. L., Suhr, O. B., Obici, L., Sekijima, Y., Zeldenrust, S. R., Yamashita, T., ... Diflunisal Trial Consortium. (2013). Repurposing diflunisal for familial amyloid polyneuropathy: a randomized clinical trial. *JAMA*, *310*(24), 2658–2667. <https://doi.org/10.1001/jama.2013.283815>
- Buxbaum, J., Anan, I., & Suhr, O. (2010). Serum transthyretin levels in Swedish TTR V30M carriers. *Amyloid*, *17*(2), 83–85.  
<https://doi.org/10.3109/13506129.2010.483118>
- Buxbaum, J. N., & Reixach, N. (2009). Transthyretin: the servant of many masters. *Cellular and Molecular Life Sciences*, *66*(19), 3095–3101.  
<https://doi.org/10.1007/s00018-009-0109-0>

- Cardoso, I., Goldsbury, C. S., Müller, S. A., Olivieri, V., Wirtz, S., Damas, A. M., ... Saraiva, M. J. (2002). Transthyretin fibrillogenesis entails the assembly of monomers: a molecular model for in vitro assembled transthyretin amyloid-like fibrils<sup>1</sup>. *Journal of Molecular Biology*, 317(5), 683–695. <https://doi.org/10.1006/jmbi.2002.5441>
- Cascella, R., Conti, S., Mannini, B., Li, X., Buxbaum, J. N., Tiribilli, B., ... Cecchi, C. (2013). Transthyretin suppresses the toxicity of oligomers formed by misfolded proteins in vitro. *Biochimica et Biophysica Acta (BBA) - Molecular Basis of Disease*, 1832(12), 2302–2314. <https://doi.org/10.1016/j.bbadis.2013.09.011>
- Chan, G. G., Koch, C. M., & Connors, L. H. (2017). Blood Proteomic Profiling in Inherited (ATTR<sub>M</sub>) and Acquired (ATTR<sub>wt</sub>) Forms of Transthyretin-Associated Cardiac Amyloidosis. *Journal of Proteome Research*. <https://doi.org/10.1021/acs.jproteome.6b00998>
- Clark, L. A. (2005). Protein aggregation determinants from a simplified model: Cooperative folders resist aggregation. *Protein Science*, 14(3), 653–662. <https://doi.org/10.1110/ps.041017305>
- Coelho, T., Maia, L. F., Silva, A. M. da, Cruz, M. W., Planté-Bordeneuve, V., Lozeron, P., ... Zibert, A. (2012). Tafamidis for transthyretin familial amyloid polyneuropathy A randomized, controlled trial. *Neurology*, 79(8), 785–792. <https://doi.org/10.1212/WNL.0b013e3182661eb1>
- Cohen, A. S., & Calkins, E. (1959). Electron microscopic observations on a fibrous component in amyloid of diverse origins. *Nature*, 183(4669), 1202–1203.
- Colon, W., & Kelly, J. W. (1992). Partial denaturation of transthyretin is sufficient for amyloid fibril formation in vitro. *Biochemistry*, 31(36), 8654–8660. <https://doi.org/10.1021/bi00151a036>
- Comenzo, R. L., Vosburgh, E., Falk, R. H., Sanchorawala, V., Reisinger, J., Dubrey, S., ... Skinner, M. (1998). Dose-Intensive Melphalan With Blood Stem-Cell Support for the Treatment of AL (Amyloid Light-Chain) Amyloidosis: Survival and Responses in 25 Patients. *Blood*, 91(10), 3662–3670. Retrieved from <http://www.bloodjournal.org/content/91/10/3662>
- Conceição, I., & De Carvalho, M. (2007). Clinical variability in type I familial amyloid polyneuropathy (Val30Met): Comparison between late- and early-onset cases in Portugal. *Muscle & Nerve*, 35(1), 116–118. <https://doi.org/10.1002/mus.20644>

- Cornwell, G., Murdoch, W., Kyle, R., Westermark, P., & Pitkanen, P. (1983). The Frequency and Distribution of Senile Cardiovascular Amyloid - a Clinicopathologic Correlation. *Clinical Research*, 31(2), A523–A523.
- de Carvalho, M., Conceição, I., Bentes, C., & Sales Luis, M. L. (2002). Long-term quantitative evaluation of liver transplantation in familial amyloid polyneuropathy (Portuguese V30M). *Amyloid*, 9(2), 126–133. <https://doi.org/10.3109/13506120208995245>
- de Larrea, C. F., Verga, L., Morbini, P., Klersy, C., Lavatelli, F., Foli, A., ... Merlini, G. (2015). A practical approach to the diagnosis of systemic amyloidoses. *Blood*, 125(14), 2239–2244. <https://doi.org/10.1182/blood-2014-11-609883>
- Dember, L. M., Hawkins, P. N., Hazenberg, B. P. C., Gorevic, P. D., Merlini, G., Butrimiene, I., ... Skinner, M. (2007). Eprodisate for the Treatment of Renal Disease in AA Amyloidosis. *New England Journal of Medicine*, 356(23), 2349–2360. <https://doi.org/10.1056/NEJMoa065644>
- Dobson, C. M. (2003). Protein folding and misfolding. *Nature*, 426(6968), 884–890. <https://doi.org/10.1038/nature02261>
- Fleming, C. E., Nunes, A. F., & Sousa, M. M. (2009). Transthyretin: More than meets the eye. *Progress in Neurobiology*, 89(3), 266–276. <https://doi.org/10.1016/j.pneurobio.2009.07.007>
- Foss, T. R., Wiseman, R. L., & Kelly, J. W. (2005). The Pathway by Which the Tetrameric Protein Transthyretin Dissociates. *Biochemistry*, 44(47), 15525–15533. <https://doi.org/10.1021/bi051608t>
- Gillmore, J. D., Lovat, L. B., Persey, M. R., Pepys, M. B., & Hawkins, P. N. (2001). Amyloid load and clinical outcome in AA amyloidosis in relation to circulating concentration of serum amyloid A protein. *The Lancet*, 358(9275), 24–29. [https://doi.org/10.1016/S0140-6736\(00\)05252-1](https://doi.org/10.1016/S0140-6736(00)05252-1)
- Giorgadze, T. A., Shiina, N., Baloch, Z. W., Tomaszewski, J. E., & Gupta, P. K. (2004). Improved detection of amyloid in fat pad aspiration: An evaluation of Congo red stain by fluorescent microscopy. *Diagnostic Cytopathology*, 31(5), 300–306. <https://doi.org/10.1002/dc.20131>
- Hammarström, P., Wiseman, R. L., Powers, E. T., & Kelly, J. W. (2003). Prevention of Transthyretin Amyloid Disease by Changing Protein Misfolding Energetics. *Science*, 299(5607), 713–716. <https://doi.org/10.1126/science.1079589>

- Hazenberg, B. P. C., van Gameren, I. I., Bijzet, J., Jager, P. L., & van Rijswijk, M. H. (2004). Diagnostic and therapeutic approach of systemic amyloidosis. *Netherlands Journal of Medicine*, *62*(4), 121–128.
- Herbert, J., Wilcox, J. N., Pham, K. T., Fremerey, R. T., Zeviani, M., Dwork, A., ... Zimmerman, E. A. (1986). Transthyretin: a choroid plexus-specific transport protein in human brain. The 1986 S. Weir Mitchell award. *Neurology*, *36*(7), 900–911.
- Herlenius, G., Wilczek, H. E., Larsson, M., & Ericzon, B. G. (2004). Ten years of international experience with liver transplantation for familial amyloidotic polyneuropathy: Results from the familial amyloidotic polyneuropathy world transplant registry. *Transplantation*, *77*(1), 64–71.  
<https://doi.org/10.1097/01.TP.0000092307.98347.CB>
- Hosoi, A., Su, Y., Torikai, M., Jono, H., Ishikawa, D., Soejima, K., ... Ando, Y. (2016). Novel Antibody for the Treatment of Transthyretin Amyloidosis. *Journal of Biological Chemistry*, *291*(48), 25096–25105.  
<https://doi.org/10.1074/jbc.M116.738138>
- Hoyer, C., Angermann, C. E., Knop, S., Ertl, G., & Störk, S. (2008). Kardiale Amyloidose. *Medizinische Klinik*, *103*(3), 153–160.  
<https://doi.org/10.1007/s00063-008-1022-2>
- Hurshman Babbes, A. R., Powers, E. T., & Kelly, J. W. (2008). Quantification of the Thermodynamically Linked Quaternary and Tertiary Structural Stabilities of Transthyretin and Its Disease-Associated Variants: The Relationship between Stability and Amyloidosis. *Biochemistry*, *47*(26), 6969–6984. <https://doi.org/10.1021/bi800636q>
- Jacobson, D. R., McFarlin, D. E., Kane, I., & Buxbaum, J. N. (1992). Transthyretin Pro55, a variant associated with early-onset, aggressive, diffuse amyloidosis with cardiac and neurologic involvement. *Human Genetics*, *89*(3), 353–356. <https://doi.org/10.1007/BF00220559>
- Johnson, S. M., Wiseman, R. L., Sekijima, Y., Green, N. S., Adamski-Werner, S. L., & Kelly, J. W. (2005). Native State Kinetic Stabilization as a Strategy To Ameliorate Protein Misfolding Diseases: A Focus on the Transthyretin Amyloidoses. *Accounts of Chemical Research*, *38*(12), 911–921.  
<https://doi.org/10.1021/ar020073i>
- Kelly, S. M., Jess, T. J., & Price, N. C. (2005). How to study proteins by circular dichroism. *Biochimica et Biophysica Acta (BBA) - Proteins and Proteomics*, *1751*(2), 119–139.  
<https://doi.org/10.1016/j.bbapap.2005.06.005>

- Kelly, S. M., & Price, N. C. (2000). The Use of Circular Dichroism in the Investigation of Protein Structure and Function. *Current Protein & Peptide Science*, 1(4), 349–384. <https://doi.org/10.2174/1389203003381315>
- Kim, Y. E., Hipp, M. S., Bracher, A., Hayer-Hartl, M., & Ulrich Hartl, F. (2013). Molecular Chaperone Functions in Protein Folding and Proteostasis. *Annual Review of Biochemistry*, 82(1), 323–355. <https://doi.org/10.1146/annurev-biochem-060208-092442>
- Kingsbury, J. S., Klimtchuk, E. S., Théberge, R., Costello, C. E., & Connors, L. H. (2007). Expression, Purification, and In Vitro Cysteine-10 Modification of Native Sequence Recombinant Human Transthyretin. *Protein Expression and Purification*, 53(2), 370–377. <https://doi.org/10.1016/j.pep.2007.01.004>
- Kon, T., Misumi, Y., Nishijima, H., Honda, M., Suzuki, C., Baba, M., ... Tomiyama, M. (2015). Effects of liver transplantation and tafamidis in hereditary transthyretin amyloidosis caused by transthyretin Leu55Pro mutation: a case report. *Amyloid*, 22(3), 203–204. <https://doi.org/10.3109/13506129.2015.1031373>
- Kyle, R. A., & Gertz, M. A. (1995). Primary systemic amyloidosis: clinical and laboratory features in 474 cases. *Seminars in Hematology*, 32(1), 45–59.
- Merlini, G., & Bellotti, V. (2003). Molecular Mechanisms of Amyloidosis. *New England Journal of Medicine*, 349(6), 583–596. <https://doi.org/10.1056/NEJMra023144>
- Munishkina, L. A., & Fink, A. L. (2007). Fluorescence as a method to reveal structures and membrane-interactions of amyloidogenic proteins. *Biochimica et Biophysica Acta (BBA) - Biomembranes*, 1768(8), 1862–1885. <https://doi.org/10.1016/j.bbamem.2007.03.015>
- Pepys, M. B. (2006). Amyloidosis. In *Annual Review of Medicine* (Vol. 57, pp. 223–241). Palo Alto: Annual Reviews.
- Petkova, A. T., Leapman, R. D., Guo, Z., Yau, W.-M., Mattson, M. P., & Tycko, R. (2005). Self-Propagating, Molecular-Level Polymorphism in Alzheimer's  $\beta$ -Amyloid Fibrils. *Science*, 307(5707), 262–265. <https://doi.org/10.1126/science.1105850>
- Robinson, L. Z., & Reixach, N. (2014). Quantification of Quaternary Structure Stability in Aggregation-Prone Proteins under Physiological Conditions: The Transthyretin Case. *Biochemistry*, 53(41), 6496–6510. <https://doi.org/10.1021/bi500739q>

- Ruberg, F. L., & Berk, J. L. (2012). Transthyretin (TTR) Cardiac Amyloidosis. *Circulation*, *126*(10), 1286–1300.  
<https://doi.org/10.1161/CIRCULATIONAHA.111.078915>
- Sekijima, Y., Tojo, K., Morita, H., Koyama, J., & Ikeda, S. (2015). Safety and efficacy of long-term diflunisal administration in hereditary transthyretin (ATTR) amyloidosis. *Amyloid*, *22*(2), 79–83.  
<https://doi.org/10.3109/13506129.2014.997872>
- Serpell, L. C., Sunde, M., Benson, M. D., Tennent, G. A., Pepys, M. B., & Fraser, P. E. (2000). The protofilament substructure of amyloid fibrils<sup>1</sup>. *Journal of Molecular Biology*, *300*(5), 1033–1039.  
<https://doi.org/10.1006/jmbi.2000.3908>
- Sharma, N., & Howlett, J. (2013). Current state of cardiac amyloidosis. *Current Opinion in Cardiology*, *28*(2), 242–248.  
<https://doi.org/10.1097/HCO.0b013e32835dd165>
- Sipe, J. D., Benson, M. D., Buxbaum, J. N., Ikeda, S.-I., Merlini, G., Saraiva, M. J. M., & Westermark, P. (2016). Amyloid fibril proteins and amyloidosis: chemical identification and clinical classification International Society of Amyloidosis 2016 Nomenclature Guidelines. *Amyloid: The International Journal of Experimental and Clinical Investigation: The Official Journal of the International Society of Amyloidosis*, *23*(4), 209–213.  
<https://doi.org/10.1080/13506129.2016.1257986>
- Skinner, M., Sancharawala, V., Seldin, D. C., Dember, L. M., Falk, R. H., Berk, J. L., ... Wright, D. G. (2004). High-Dose Melphalan and Autologous Stem-Cell Transplantation in Patients with AL Amyloidosis: An 8-Year Study. *Annals of Internal Medicine*, *140*(2), 85–93.  
<https://doi.org/10.7326/0003-4819-140-2-200401200-00008>
- Sousa, J. C., Grandela, C., Fernández-Ruiz, J., De Miguel, R., De Sousa, L., Magalhães, A. I., ... Palha, J. A. (2004). Transthyretin is involved in depression-like behaviour and exploratory activity. *Journal of Neurochemistry*, *88*(5), 1052–1058. <https://doi.org/10.1046/j.1471-4159.2003.02309.x>
- Sousa, J. C., Marques, F., Dias-Ferreira, E., Cerqueira, J. J., Sousa, N., & Palha, J. A. (2007). Transthyretin influences spatial reference memory. *Neurobiology of Learning and Memory*, *88*(3), 381–385.  
<https://doi.org/10.1016/j.nlm.2007.07.006>

- Sousa, M. M., Fernandes, R., Palha, J. A., Taboada, A., Vieira, P., & Saraiva, M. J. (2002). Evidence for Early Cytotoxic Aggregates in Transgenic Mice for Human Transthyretin Leu55Pro. *The American Journal of Pathology*, 161(5), 1935–1948. [https://doi.org/10.1016/S0002-9440\(10\)64469-0](https://doi.org/10.1016/S0002-9440(10)64469-0)
- Stefani, M. (2008). Protein Folding and Misfolding on Surfaces. *International Journal of Molecular Sciences*, 9(12), 2515. <https://doi.org/10.3390/ijms9122515>
- Tanskanen, M., Peuralinna, T., Polvikoski, T., Notkola, I., Sulkava, R., Hardy, J., ... Myllykangas, L. (2008). Senile systemic amyloidosis affects 25% of the very aged and associates with genetic variation in alpha2-macroglobulin and tau: A population-based autopsy study. *Annals of Medicine*, 40(3), 232–239. <https://doi.org/10.1080/07853890701842988>
- Tojo, K., Sekijima, Y., Kelly, J. W., & Ikeda, S. (2006). Diflunisal stabilizes familial amyloid polyneuropathy-associated transthyretin variant tetramers in serum against dissociation required for amyloidogenesis. *Neuroscience Research*, 56(4), 441–449. <https://doi.org/10.1016/j.neures.2006.08.014>
- Virchow VR. Ueber einem Gehirn and Rueckenmark des Menchen auf gefundene Substanz mit chemischen reaction der Cellulose. *Virchow's Archive: Pathological Anatomy*. 1854; 6:135-138
- Wechalekar, A. D., Gillmore, J. D., & Hawkins, P. N. (2016). Systemic amyloidosis. *The Lancet*, 387(10038), 2641–2654. [https://doi.org/10.1016/S0140-6736\(15\)01274-X](https://doi.org/10.1016/S0140-6736(15)01274-X)
- Westermarck, P., Sletten, K., Johansson, B., & Cornwell, G. G. (1990). Fibril in senile systemic amyloidosis is derived from normal transthyretin. *Proceedings of the National Academy of Sciences*, 87(7), 2843–2845. Retrieved from <http://www.pnas.org/content/87/7/2843>

## CURRICULUM VITAE

